Mnt-Deficient Mammary Glands Exhibit Impaired Involution and Tumors with Characteristics of Myc Overexpression

Kazuhito Toyo-oka,[1] Timothy J. Bowen,[1] Shinji Hirotsune,[7] Zirong Li,[2,3] Sonia Jain,[4] Sara Ota,[8] Laure Escoubet Lozach,[2] Ivan Garcia Bassett,[5] Jean Lozach,[2] Michael G. Rosenfeld,[5,6] Christopher K. Glass,[8] Robert Eisenman,[9] Bing Ren,[2,3] Peter Hurlin,[8] and Anthony Wynshaw-Boris[1]

[1]Departments of Pediatrics and Medicine, University of California, San Diego Comprehensive Cancer Center; [2]Department of Cellular and Molecular Medicine, Ludwig Cancer Institute; [3]Ludwig Cancer Institute; [4]Department of Family and Preventive Medicine, Division of Biostatistics and Bioinformatics; [5]Department of Medicine; and [6]Howard Hughes Medical Institute, University of California, San Diego School of Medicine, La Jolla, California; [7]Division of Genetic Disease Research, Graduate School of Medicine, Osaka City University, Abeno, Osaka, Japan; [8]Department of Cell and Developmental Biology, Shriners Hospitals for Children, Oregon Health Sciences University, Portland, Oregon; and [9]Division of Basic Sciences, Fred Hutchinson Cancer Research Center, Seattle, Washington

Abstract

The proto-oncogene c-Myc plays a central role in cell growth and the development of human tumors. c-Myc interacts with Max and Myc-Max complexes bind to E-box and related sequences to activate transcription. Max also interacts with Mnt but Mnt-Max complexes repress transcription when bound to these sequences. *MNT* maps to human chromosome 17p13.3, a region frequently deleted in various human tumors, including mammary gland tumors. Consistent with the possibility that Mnt functions as a Myc antagonist, Mnt-deficient fibroblasts exhibit many of the hallmark characteristics of cells that overexpress Myc, and conditional (Cre/Lox) inactivation of *Mnt* in mammary gland epithelium leads to adenocarcinomas. Here, we further characterize mammary gland tissue following conditional deletion of Mnt in the mammary gland. We show that loss of *Mnt* severely disrupts mammary gland involution and leads to hyperplastic ducts associated with reduced numbers of apoptotic cells. These findings suggest that loss of Mnt in mammary tissue has similarities to Myc overexpression. We tested this directly by using promoter array analysis and mRNA expression analysis by oligonucleotide arrays. We found that Mnt and c-Myc bound to similar promoters in tumors from *MMTV-c-Myc* transgenic mice, and mRNA expression patterns were similar between mammary tumors from *MMTV-Cre/Mnt$^{KO/CKO}$* and *MMTV-c-Myc* transgenic mice. These results reveal an important role for *Mnt* in pregnancy-associated mammary gland development and suggest that mammary gland tumorigenesis in the absence of Mnt is analogous to that caused by Myc deregulation. (Cancer Res 2006; 66(11): 5565-73)

Introduction

Myc family proteins are nuclear phosphoproteins that play a pivotal role in many cellular events, including the control of cell growth, proliferation, differentiation, and embryonic development (reviewed in ref. 1). Moreover, it is well known that the dysregulation of c-Myc is associated with tumorigenesis in a variety of contexts (reviewed in ref. 2). In many tumors and tumor-derived cell lines, *myc* genes are altered by gene amplification, chromosome translocations, and viral insertion, events that typically lead to deregulation of Myc with increased Myc expression (reviewed in ref. 2). The relevance of these alterations to tumorigenesis is suggested by the ability of forced overexpression of Myc *in vivo* to cause tumors in a wide variety of tissues, including mammary gland epithelium (3–5).

The Myc family of proteins (c-Myc, N-Myc, and L-Myc) require heterodimerization with Max through related bHLHZip motifs to bind DNA and function as transcription factors (1). Max also interacts with the four Mxd (formerly Mad) family members, Mad1, Mxi1, Mad3, and Mad4, as well as the Mad-related proteins Mnt and Mga, to form heterodimers via bHLHZip domains (reviewed in ref. 1). As with Myc, heterodimerization with Max allows these proteins to bind the E-box consensus sequence, CACGTG, and related sequences. The Mad family, Mnt and Mga, are transcriptional repressors that can compete with Myc for binding to Max, and it is hypothesized that all of these complexes can compete for binding to shared target sites *in vivo* (1). Recent experiments showing that Mnt-Max complexes decline when c-Myc is induced during cell cycle entry also suggest that Mnt and c-Myc compete for binding for a limiting supply of Max (6). Thus, activating Myc-Max complexes together with repressive Mnt-Max, Mad-Max, and Mga-Max complexes seem to function as an antagonistic network through the binding and transcriptional regulation of shared target genes.

The *MNT* gene maps to human 17p13.3, a region that is commonly deleted in a variety of tumors, including mammary gland tumors (7–10). Although no mutations in *MNT* have been described in human tumors to date (11–13), previous studies have shown that frequent loss of heterozygosity (LOH) in 17p13.33, but also in 17p25.1, 8p22, 13q12, and 22q13, correlates with postoperative recurrence in breast cancers (14). LOH involves a region telomeric to p53 at 17p13.1 (14) and clearly indicates the presence of another tumor suppressor gene(s) located in 17p13.3. A candidate tumor suppressor gene in this region is *HIC1* (hypermethylated in cancer), which is aberrantly hypermethylated and transcriptionally inactivated in several types of human cancers (15–17). Heterozygous *Hic1* mutant mice have no developmental phenotype but are predisposed to malignant tumors, including pulmonary carcinomas, lymphomas, and sarcomas (18). However, these mice do not display mammary gland cancer, suggesting that candidate tumor suppressor genes within 17p13.3 responsible for

Note: Supplementary data for this article are available at Cancer Research Online (http://cancerres.aacrjournals.org/).

Requests for reprints: Anthony Wynshaw-Boris, Departments of Pediatrics and Medicine, University of California, San Diego, Medical Teaching Facility, Room 253, 9500 Gilman Drive, MC 0627, La Jolla, CA 92093-0627. Phone: 858-822-3400; Fax: 858-822-3409; E-mail: awynshawboris@ucsd.edu.

doi:10.1158/0008-5472.CAN-05-2683

other malignant tumors, such as breast tumors, remain to be identified. A recent study suggests that MNT is a potential tumor suppressor gene in medulloblastoma (19). Chromosome 17p13.3 is also well defined as the Miller-Dieker syndrome critical region. Patients with Miller-Dieker syndrome display severe neuronal migration defects defined by lissencephaly (smooth brain) as well as dysmorphic features consistent with abnormalities in craniofacial development (reviewed in ref. 20).

We recently showed that loss of *Mnt* causes a hyperproliferation phenotype in mouse embryonic fibroblasts, including accelerated proliferation, increased sensitivity to apoptosis, sensitivity to transformation by H-Ras^{V12} alone, and senescence bypass (ref. 21; also reviewed in ref. 22). In addition, conditional deletion of *Mnt* in mouse mammary gland epithelium led to the development of mammary adenocarcinomas after long latency. *Mnt*-deficient fibroblasts and mammary gland epithelium displayed decreased c-Myc, but increased cyclin E and cyclin-dependent kinase (Cdk)-4, consistent with a phenotype resulting from increased relative c-Myc activity. Here we extend these findings to show that loss of Mnt in mammary gland epithelium causes defects in mammary gland development and severely disrupts involution. We also used genome-wide location analysis (GWLA) to examine promoter binding of c-Myc and Mnt in tumors arising from overexpression of c-Myc, and oligonucleotide expression arrays to compare mRNA expression patterns between tumors resulting from loss of Mnt or overexpression of c-Myc. Our results indicate an important role for Mnt in mammary gland development and suggest that tumorigenesis caused by loss of Mnt and overexpression of c-Myc are functionally related.

Materials and Methods

Generation of Mnt mutant mice. The production of mice with a *Mnt* conditional knockout (Mnt^{CKO}) allele by gene targeting is described elsewhere (23). Briefly, a *loxP*-flanked *hygro* resistance gene and third *loxP* were inserted into introns 3 and 6, respectively, of the *Mnt* gene by gene targeting. EIIa-Cre transgenic mice in an FVB/n background (24) were mated with inbred 129/S6 $Mnt^{+/CKO}$ mice to generate the Mnt^{KO} allele in a mixed background (129/S6 × FVB/n) mice *in vivo*. To produce mice with loss of *Mnt* in the mammary gland (*MMTV-Cre*$^+$/$Mnt^{KO/CKO}$ mice), *MMTV-Cre* mice were mated with $Mnt^{+/KO}$ mice to produce *MMTV-Cre*$^+$/$Mnt^{KO/+}$ mice. *MMTV-Cre*$^+$/$Mnt^{KO/CKO}$ mice were produced by breeding *MMTV-Cre*$^+$/$Mnt^{KO/+}$ mice with $Mnt^{CKO/CKO}$ mice. We used *MMTV-Cre*$^-$/$Mnt^{KO/CKO}$ mice without *MMTV-Cre* as control. *MMTV-Cre*$^-$/$Mnt^{KO/CKO}$ mice displayed no mammary gland tumors.

Genotyping analysis. Adult mice were genotyped by PCR analysis using tail DNA. The following primers were used to detect wild-type, conditional, or deleted allele. MntWT-sense (5′-cagtccctgaagaggaagga-3′) and MntWT-Rev2 (5′-ccggagcacacgatctatct-3′) were employed for wild-type allele detection. MntKO3 (5′-caggtcctccaaaagagcag-3′) and MntKO4 (5′-ggagcaatgtggagagaagc-3′) were used for deleted allele detection. The conditions of amplification were 35 cycles at 94°C for 30 seconds, 68°C for 60 seconds, and 72°C for 120 seconds. This PCR reaction generates a 386-bp fragment from mutant allele and a 147-bp from wild-type allele. To distinguish wild-type and conditional mutant alleles, two primers (sense, 5′-cagattcagtgtcccctgct-3′; antisense, 5′-gtctcaagtcgtgggcattg-3′) were used to amplify a 178-bp product from the wild-type allele and a 1.9-kbp product from the conditional allele. The results from this PCR were confirmed by detection of the *hygro* resistance gene with primers for *hygro* (sense, 5′-gatgtaggagggcgtggata-3′; antisense, 5′-gatgttggcgacctcgtatt-3′). The *MMTV-Cre* allele was detected with the primers CREA1 (5′-ccgggctgccacgaccaa-3′) and CREA2 (5′-ggcgcggcaacaccatttttt-3′).

Whole-mount analysis of mammary gland. Mammary gland tissues were dissected at various developmental stages from the two genotypes (*MMTV-Cre*$^+$/$Mnt^{KO/CKO}$ and *MMTV-Cre*$^-$/$Mnt^{KO/CKO}$), spread on glass slides, and fixed immediately with Carnoy's fixative (6 volumes ethanol; 4 volumes chloroform; 1 volume acetic acid) for 5 hours at room temperature. After 3 days of acetone treatment to remove lipid, tissues were hydrated with serially diluted ethanol. Hydrated tissues were stained with 0.6% carmine solution for 1 hour at room temperature, followed by treatment with differentiating solution (36% ethanol, 18% methanol). Dehydrated tissues with ethanol were cleared with benzyl alcohol/benzyl benzoate (1:2) solution.

Histologic analysis. Mammary gland tissues (n = 4-5 for each genotype) were dissected at various stages and fixed in 4% paraformaldehyde/PBS solution for 15 hours at 4°C. Fixed tissues were embedded in paraffin, sectioned at 5 μm, and stained with H&E.

Terminal deoxyribonucleotidyl transferase–mediated dUTP nick end labeling analysis in the developing mammary gland. Mammary gland tissues fixed with 4% paraformaldehyde/PBS were embedded in paraffin, sectioned at 5 μm, and deparaffinized. Apoptotic cells were detected by using the ApopTag kit (Intergen Company, Purchase, NY) according to the instructions of the manufacturer. For quantification analysis, terminal deoxyribonucleotidyl transferase–mediated dUTP nick end labeling (TUNEL)–positive cells in 100 × 150-μm area were counted in both *MMTV-Cre*$^+$/$Mnt^{KO/CKO}$ mice and *MMTV-Cre*$^-$/$Mnt^{KO/CKO}$ mice.

Western blot analysis. Tumors and adjacent normal tissue from *MMTV-Cre*$^+$/$Mnt^{KO/CKO}$ or from wild-type C57/Bl6 mice were dissected and lysates were prepared as previously described for Western blotting (25). Antibodies against Mnt and c-myc were used as previously described (26).

Kaplan-Meier analysis. To analyze mammary gland tumor development of *MMTV-Cre*$^+$/$Mnt^{KO/CKO}$ mice, we longitudinally followed 10 *MMTV-Cre*$^+$/$Mnt^{KO/CKO}$ mice and 9 *MMTV-Cre*$^-$/$Mnt^{KO/CKO}$ mice as controls. All mice were checked weekly for mammary gland tumor development by palpation and mice were sacrificed when they displayed a 1-cm mammary gland tumor. The time from birth was plotted on the X axis and mammary gland tumor-free survival (as percentage of total number of mice) was plotted on the Y axis. The censored subjects are shown as solid squares or triangles in the horizontal part of the staircase and include all deaths not associated with mammary gland tumors.

Statistical analysis. H&E-stained sections (five to seven sections per mouse) of mammary gland for each developmental stage were used to determine the ductal area by using Microanalyzer software (Nihon Poladigital, Tokyo, Japan). The percentage of enlarged ducts was calculated on the basis of the measurement of ductal area. "Enlarged duct" was defined as the ducts in which the area was larger than the area of wild-type (the average area of wild-type was 1,500 μm^2). Statistical significance was determined by two-sided Student's t test.

Preparation of chromatin for microarray analysis. A DNA microarray containing PCR products spanning the proximal promoters of 1,920 mouse genes (M2K, Supplementary Table S1) was chosen from the NCBI Refseq database. These genes were selected for good gene annotation and a clear functional association. Tumors were harvested and cross-linked in formaldehyde [11% formaldehyde/0.1 mol/L NaCl/1 mmol/L Na-EDTA/0.5 mmol/L Na-EGTA/50 mmol/L HEPES (pH 8.0)] and incubated on ice for 10 minutes. The cross-linking reaction was stopped with a 1/20 volume of 2.5 mol/L glycine solution. Following cross-linking, chromatin was extracted in lysis buffer [0.2 mol/L NaCl/1 μmol/L EDTA/0.5 μmol/L EGTA/10 μmol/L Tris (pH 8)/protease inhibitor cocktail] for 10 minutes, followed by centrifugation at 2,000 × g for 10 minutes at 4°C.

Chromatin was fragmented using sonication on ice and immunoprecipitated using magnetic beads coupled to primary antibodies to *c-Myc* and *Mnt* as described (27). The beads were collected and the supernatant was removed. The chromatin was eluted from the beads using elution buffer [50 mmol/L Tris (pH 8)/10 mmol/L EDTA/1% SDS]. The cross-link was reversed and DNA was purified and prepared for labeling and microarray hybridization through random primer amplification. The samples were then hybridized to the M2K Microarray slides and analyzed using previously described protocols (28). The antibodies to c-Myc (28) and Mnt (6) have been validated previously for chromatin immunoprecipitation. To validate the array data, genomic sequence primers encompassing *Ibd1, Sap18,*

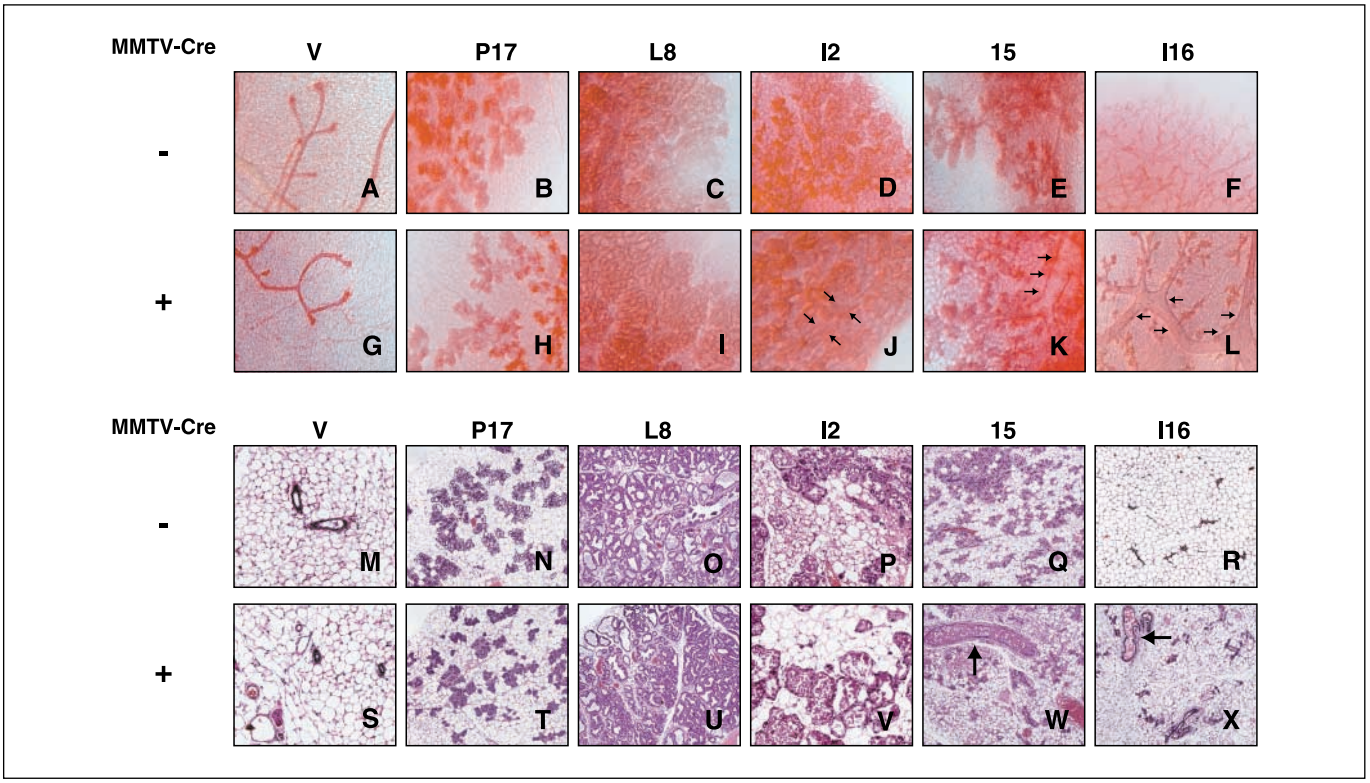

Figure 1. Morphologic analysis by whole-mount analysis (*A-L*) and histologic sections with H&E staining (*M-X*) of developing mammary gland in *MMTV-Cre*$^{-}$/*Mnt*$^{KO/CKO}$ mice (*A-F, M-R*) and *MMTV-Cre*$^{+}$/*Mnt*$^{KO/CKO}$ mice (*G-L, S-X*). Note the enlarged ducts in *MMTV-Cre*$^{+}$/*Mnt*$^{KO/CKO}$ mice (*J-L, W*, and *X, arrows*). *V,* virgin; *P17,* 17 days of pregnancy; *L8,* 8 days of lactation; *I2, I5,* and *I16,* 2, 5, and 16 days after removal of pups after 12 days of lactation.

Cdkn1b, Rab18, and *Brca1* promoter regions that bound Mnt and c-myc were used to amplify immunoprecipitated DNA. The following primers, corresponding to promoter regions of each gene, were used for the chromatin immunoprecipitation analysis: *Ibd1* sense 5′-CACCTGGGGTCAGAACATCT-3′, antisense 5′-CTGTTGGAAGATTGGGCTGT-3′; *Sap18* sense 5′-CCTTGCCACTCGTTTCCTAT-3′, antisense 5′-CCGGCTCCTTCTTAATTTCC-3′; *Cdkn1b* sense 5′-CTAGCCACCGAAGCTCCTAA-3′, antisense 5′-GCCCCGGAGAAATTAAAAAT-3′; *Rab18* sense 5′-TGATGTGGGGAGACACTTGA-3′, antisense 5′-GGCAGAGCTGCTGTAAATCC-3′; and *Brca1* sense 5′-TCCGGTGTGAGAAGCTCTTT-3′, antisense 5′-AGCAGTTGCAAAACGAGGTC-3′. The following primers, corresponding to intragenic regions of each gene, were used as negative control: *Ibd1* sense 5′-GCCTCCAAACTTTTGCTGAG-3′, antisense 5′-CTGCAGAGGCTAGGATACCG-3′; *Sap18* sense 5′-TGAGAGGGGCTAAGAGGTGA-3′, antisense 5′-GTCCTCAAAATCAGGGCAAA-3′; *Cdkn1b* sense 5′-TGTCCTCCTAATGGCAAAGG-3′, antisense 5′-TGGCAGTGGGAATGTAGTCA-3′; *Rab18* sense 5′-GCAATTGTCTGGCTGTGAGA-3′, antisense 5′-AAAGGCCTGAAGGGGTTAGA-3′; and *Brca1* sense 5′-CAGGTCAGCTACCACAGCAA-3′, antisense 5′-TTGGACATTGTGGAGCTTGA-3′.

Expression arrays analysis. Expression microarrays were done on the Affymetrix 430 2.0 mouse microarray chips. This chipset represents some 45,000 genes and single-nucleotide polymorphisms from the mouse genome. Total RNA was isolated from two *Mnt*$^{KO/CKO}$*; MMTV-Cre* mammary tumors and two *c-Myc* transgenic mammary tumors. The RNA was labeled and hybridized to the array using standard protocols. Microarray data were preprocessed via the Robust Multichip Average method (29) as implemented in Bioconductor,[10] a suite of programs for the R statistical programming language.[11] Robust Multichip Average preprocessing consists of three steps: background adjustment, normalization, and summarization (29). Analysis of expression was done using bioweight analysis (30). Bioweight is designed to produce a higher true positive rate compared with traditionally used *t* test– and *P* value–based methods of analysis, especially for smaller sample sets. Bioweight takes into consideration the across-replicate effect of traditional fold change analysis as well as the negative decimal log of *P* values for the gene specific *t* tests. This method allows the user to retain overexpressed/underexpressed genes that may be of biological significance as well as retain statistical stringency corresponding to a small *P* value. Therefore, the bioweight value can be described as the product of absolute average fold change and negative log of *P* value, accounting for small *P* values and large fold changes and providing a smooth transition between the two. For a detailed explanation of bioweight analysis, see Rosenfeld et al. (30).

[10] Bioconductor: http://www.bioconductor.org/.
[11] R Project for Statistical Computing: http://www.r-project.org/.

Results

Morphologic analysis of mammary gland development. To determine if loss of *Mnt* in the mammary gland was associated with developmental abnormalities, we analyzed mammary gland development during pregnancy, lactation, and involution in *MMTV-Cre*$^{+}$/*Mnt*$^{KO/CKO}$ mice and *MMTV-Cre*$^{-}$/*Mnt*$^{KO/CKO}$ control mice by whole-mount (Fig. 1*A-L*) and histologic sections (Fig. 1*M-X*). Virgin mammary glands (V, Fig. 1*A, G* and *M, S*) and mammary gland development during pregnancy (P17, Fig. 1*B, H* and *N, T*) and during and lactation (L8, Fig. 1*C, I* and *O, U*) were indistinguishable between genotypes. However, mammary glands from *MMTV-Cre*$^{+}$/*Mnt*$^{KO/CKO}$ mice displayed defects characterized by enlarged ducts during involution after weaning (arrows in Fig. 1*J, K, L, W, X*). In control mice, involution was advanced between 2 days postweaning (I2, 2 days after removal of pups; Fig. 1*D* and *P*) and 5 days

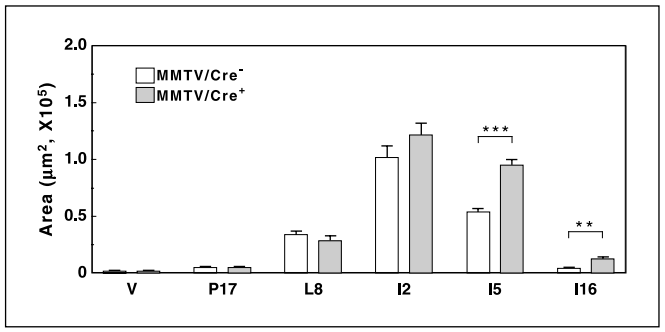

Figure 2. Quantification of the ductal area in developing mammary glands from *MMTV-Cre*$^{-}$*/Mnt*$^{KO/CKO}$ mice (*white columns; n* = 3 for each stage) and *MMTV-Cre*$^{+}$*/Mnt*$^{KO/CKO}$ mice (*gray columns; n* = 3-4 for each stage). *Columns,* mean; *bars,* SD. **, $P < 0.01$; ***, $P < 0.001$.

postweaning (I5, 5 days after removal of pups; Fig. 1*E* and *Q*) whereas the mammary gland epithelial tree was greatly reduced by day 16 (I16, 16 days after removal of pups; Fig. 1*F* and *R*). By contrast, in *MMTV-Cre*$^{+}$*/Mnt*$^{KO/CKO}$ mice, involution was delayed at I2 (Fig. 1*J* and *V*), I5 (Fig. 1*K* and *W*), and I16 (Fig. 1*L* and *X*) postweaning compared with controls. At the end of involution, the ducts of *MMTV-Cre*$^{+}$*/Mnt*$^{KO/CKO}$ mice were still enlarged in comparison with those of *MMTV-Cre*$^{-}$*/Mnt*$^{KO/CKO}$ mice (Fig. 1*L* and *X, arrows*). These changes were quantitated by calculating the area of ducts in histologic sections (Fig. 2), showing significant differences between genotypes at I5 and I15.

Reduced apoptosis during involution of the postlactation mammary gland. As involution occurs predominantly by apoptosis, we did TUNEL analysis on sections from involution days 2, 5, and 16 (I2, I5, and I16). In *MMTV-Cre*$^{-}$*/Mnt*$^{KO/CKO}$ mammary alveoli, apoptosis peaked at involution day 2 (Fig. 3*A, C*, and *E*). In contrast, apoptosis peaked at involution day 5 in *MMTV-Cre*$^{+}$*/Mnt*$^{KO/CKO}$ mice (Fig. 3*B, D*, and *F*). The percentage of TUNEL^{+} cells was calculated in alveoli (Fig. 3*G*) and ducts (Fig. 3*H*), respectively. In alveoli, the peak level of apoptosis in *MMTV-Cre*$^{+}$*/Mnt*$^{KO/CKO}$ mice was delayed compared with *MMTV-Cre*$^{-}$*/Mnt*$^{KO/CKO}$ mice (Fig. 3*G*). In addition, a decreased number of apoptotic cells were observed in the ducts of *MMTV-Cre*$^{+}$*/Mnt*$^{KO/CKO}$ mice (Fig. 3*H*). These results are consistent with an important function for Mnt in the regulation of apoptosis in both alveoli and ducts during involution.

Accumulated apoptotic defects resulted in the enlargement of mammary ducts. We calculated the percentage of enlarged ducts (Fig. 4*A*) and average area of ducts in aged virgin female mice (Fig. 4*B*) and aged nonvirgin female mice that had undergone multiple (6–8) pregnancies (Fig. 4*C*). Nonvirgin *MMTV-Cre*$^{+}$*/Mnt*$^{KO/CKO}$ mice displayed ~90% enlarged ducts in comparison with *MMTV-Cre*$^{-}$*/Mnt*$^{KO/CKO}$ mice, which had only 40% enlarged ducts, and virgin *MMTV-Cre*$^{-}$*/Mnt*$^{KO/CKO}$ mice and *MMTV-Cre*$^{+}$*/Mnt*$^{KO/CKO}$ mice, which showed 30% and 50% enlarged ducts, respectively. The enlargement of ductal area is obvious in mammary glands after multiple pregnancies (Fig. 4*C*) in comparison with virgin mice (Fig. 4*B*). These results strongly suggest that the high percentage of enlarged ducts in nonvirgin *MMTV-Cre*$^{+}$*/Mnt*$^{KO/CKO}$ mice results from accumulation of ductal material due to decreased apoptosis during successive involutions postpregnancy.

c-Myc and Mnt expression during mouse mammary gland development. To support the notion that Mnt is essential for mammary gland development during pregnancy, lactation, and involution, we analyzed Mnt and c-Myc expression by Western blotting (Fig. 5). Mnt was detectable at different stages during mammary gland development in *MMTV-Cre*$^{+}$*/Mnt*$^{KO/CKO}$ mice but its expression did show small fluctuations. In *MMTV-Cre*$^{+}$*/Mnt*$^{KO/CKO}$ mice, Mnt expression was strongly reduced as expected. Compared with Mnt, c-Myc expression was highly variable during mammary gland development. c-Myc increased in *MMTV-Cre*$^{+}$*/Mnt*$^{KO/CKO}$ mice during pregnancy, whereas during involution, there was a reduction then an increase in c-Myc. Similar changes in c-Myc were observed in *MMTV-Cre*$^{+}$*/Mnt*$^{KO/CKO}$ mice. These results suggest that reduced expression of Mnt causes an imbalance of c-Myc expression, and this may be one cause of mammary tumor development in *MMTV-Cre*$^{+}$*/Mnt*$^{KO/CKO}$ mice.

Mammary gland–specific loss of *Mnt* results in mammary adenocarcinoma. As previously described (21), we used *MMTV-Cre* mice (31, 32) to produce 11 *MMTV-Cre*$^{+}$*/Mnt*$^{KO/CKO}$ mice that were continuously mated to promote loss of *Mnt* specifically in mammary gland epithelial cells. Nine continuously mated female *MMTV-Cre*$^{-}$*/Mnt*$^{KO/CKO}$ mice were used as controls. Here we

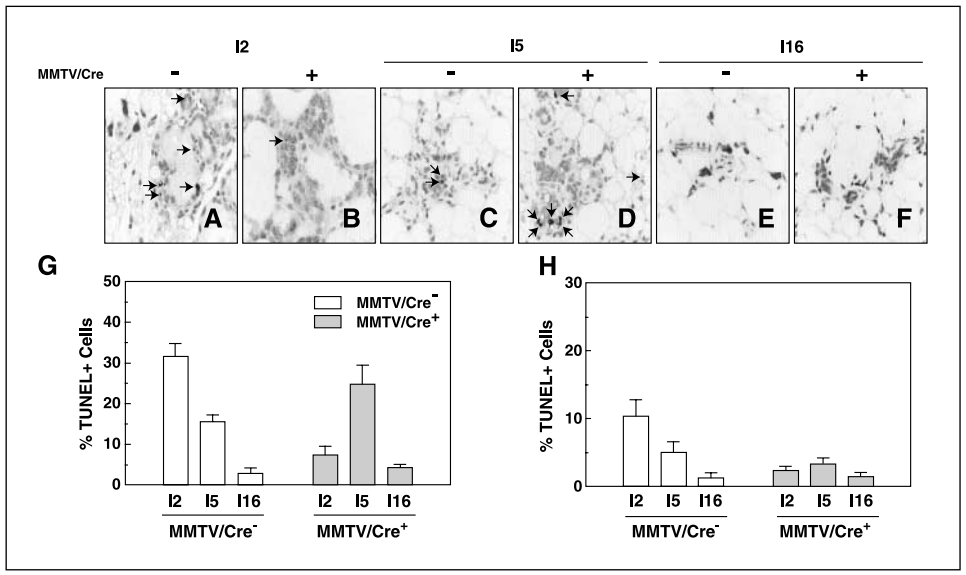

Figure 3. Apoptotic defects during involution in *MMTV-Cre*$^{+}$*/Mnt*$^{KO/CKO}$ mice. *A-F,* TUNEL staining was done on sections of mammary gland of *MMTV-Cre*$^{-}$*/Mnt*$^{KO/CKO}$ mice (*A, C*, and *E; n* = 3 for each stage) and *MMTV-Cre*$^{+}$*/Mnt*$^{KO/CKO}$ mice (*B, D*, and *F; n* = 3 for each stage) on involution day 2 (*A* and *B*), day 5 (*C* and *D*), and day 16 (*E* and *F*). Magnification, × 400. *G* and *H,* quantification of TUNEL^{+} cell in alveoli (*G*) and ducts (*H*) of *MMTV-Cre*$^{-}$*/Mnt*$^{KO/CKO}$ mice (*white columns*) and *MMTV-Cre*$^{+}$*/Mnt*$^{KO/CKO}$ mice (*solid columns*). Note delayed apoptosis in alveoli of *MMTV-Cre*$^{+}$*/Mnt*$^{KO/CKO}$ mice and decreased number of apoptosis in those ducts. *Columns,* mean; *bars,* SD.

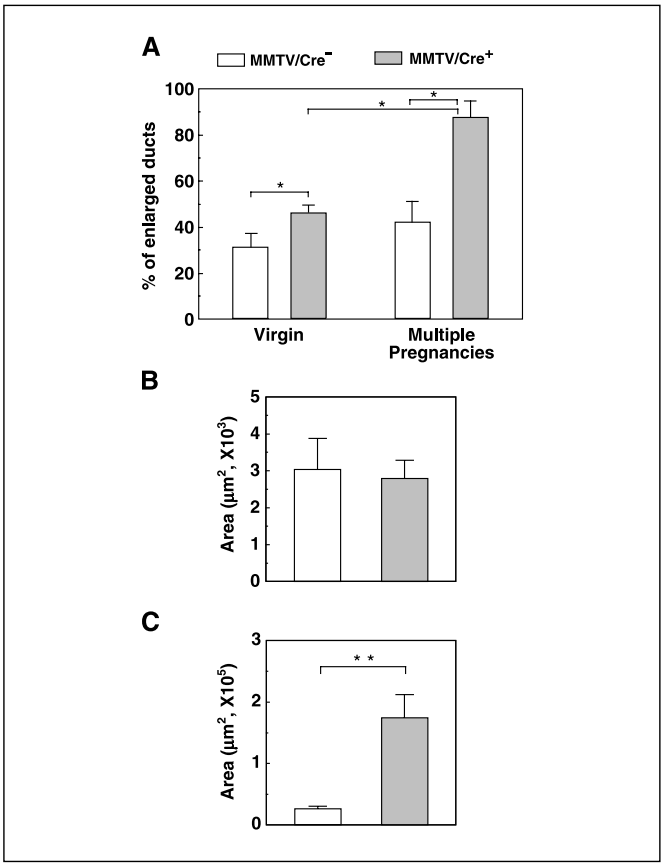

Figure 4. Multiple pregnancies accelerate the ductal enlargement. *A,* percentage of enlarged ducts in *MMTV-Cre*$^{-}$*/Mnt*$^{KO/CKO}$ mice and *MMTV-Cre*$^{+}$*/Cre*$^{+}$*/Mnt*$^{KO/CKO}$ virgin mice or mice that have had multiple pregnancies. *B* and *C,* ductal area in *MMTV-Cre*$^{-}$*/Mnt*$^{KO/CKO}$ mice (*white boxes*) and *MMTV-Cre*$^{+}$*/Mnt*$^{KO/CKO}$ mice (*shaded boxes*) that are virgin (*B; n* = 4 for each genotype) or have had multiple pregnancies (*C; n* = 5 for each genotype). *Columns,* mean; *bars,* SD. *, $P < 0.05$; **, $P < 0.01$.

present further details of the mammary gland tumor phenotype of these mice, including Kaplan-Meier survival analysis and a more complete histologic analysis of tumors.

Seven of eleven *MMTV-Cre*$^{+}$*/Mnt*$^{KO/CKO}$ mice developed mammary adenocarcinomas (Fig. 6*A*). Tumor latency ranged from 6 to 24 months (Fig. 6*B*). No tumors were observed in *MMTV-Cre*$^{-}$*/Mnt*$^{KO/CKO}$ mice (Fig. 6*A*) and mammary gland morphology was

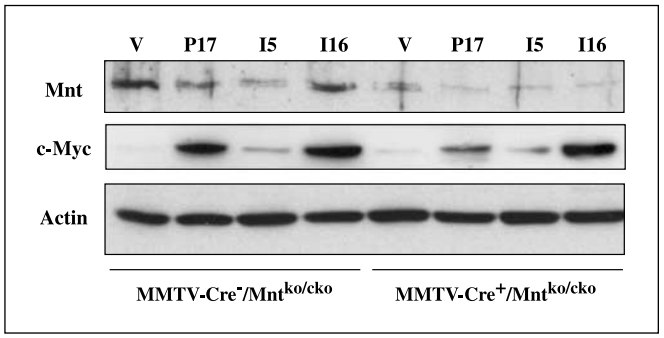

Figure 5. Western blot analysis of Mnt and c-Myc expression during pregnancy, lactation, and involution. Protein lysates from *MMTV-Cre*$^{-}$*/Mnt*$^{KO/CKO}$ mice (*lanes 1-4*) and *MMTV-Cre*$^{+}$*/Mnt*$^{KO/CKO}$ mice (*lanes 5-8*) were analyzed by Western blot for the expression levels of Mnt and c-Myc. β-Actin was used as a loading control.

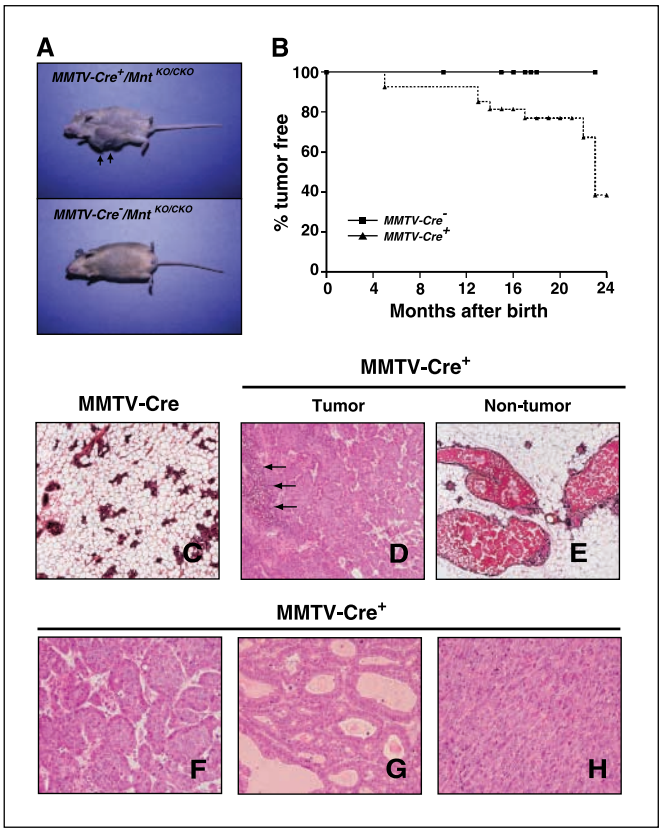

Figure 6. Mammary gland tumor development in *MMTV-Cre*$^{+}$*/Mnt*$^{KO/CKO}$ mice. *A,* mammary gland tumor was developed in 22-month-old *MMTV-Cre*$^{+}$*/Mnt*$^{KO/CKO}$ mice (*top*) compared with age-matched control *MMTV-Cre*$^{-}$*/Mnt*$^{KO/CKO}$ mice (*bottom*). *B,* incidence of mammary gland tumors in *MMTV-Cre*$^{+}$*/Mnt*$^{KO/CKO}$ mice (*dotted line*) and *MMTV-Cre*$^{-}$*/Mnt*$^{KO/CKO}$ mice (*solid line*). *MMTV-Cre*$^{+}$*/Mnt*$^{KO/CKO}$ mice and *MMTV-Cre*$^{-}$*/Mnt*$^{KO/CKO}$ mice were monitored over a period of 24 months. *D,* carcinoma with lymphocyte infiltration (*arrows*). Magnification, ×200. *E,* enlarged ducts. *F,* solid tubular carcinoma. *G,* tubular carcinoma. *H,* carcinoma with sarcomatous change. Note that *MMTV-Cre*$^{+}$*/Mnt*$^{KO/CKO}$ mice develop some different types of mammary adenocarcinomas (*F-H*) and have enlarged ducts (*E*) compared with age-matched *MMTV-Cre*$^{-}$*/Mnt*$^{KO/CKO}$ mice (*C*). Magnification, ×200 (*D*), ×400 (*C* and *E-H*).

normal in these mice (Fig. 6*C*). Some of the tumors showed lymphocyte invasion (Fig. 6*D*). The tumors were invasive ductal carcinoma with varying histology, including solid tubular carcinoma (Fig. 6*F*), tubular carcinoma (Fig. 6*G*), and carcinoma with sarcomatous change (Fig. 6*H*). In areas adjacent to the tumors, the nontumor tissue seemed to display enlarged ductal morphology although we cannot rule out that such areas were early preneoplastic lesions (Fig. 6*E*).

Mnt and Myc bind similar promoters. The notion that Mnt may act as a counterregulator of c-Myc predicts that c-Myc and Mnt bind to similar sequences in the promoter regions of regulated genes by competitively binding to those locations. To assess this hypothesis, Genome Wide Location Analysis (GWLA) was used to determine if c-Myc and Mnt have similar promoter occupancy in *MMTV-c-Myc* transgenic mammary tumors (33). One *Mnt* and two independent *c-Myc* location-analysis experiments were done on a M2K microarray chip containing ~2,000 mouse gene promoters (Supplementary Table S1) as previously described (28). The *P* value was set at <0.001 to maintain a strict stringency for comparisons of promoter binding, and Mnt and Myc bound to a very similar set of genes by these strict criteria.

Promoter DNA sequences that coimmunoprecipitated with *Mnt* were rank ordered by their *P* value for binding affinity versus control, unenriched chromatin DNA. After this rank order was established, promoters that coprecipitated with *c-Myc* were aligned with the established order to determine if there was a similarity in *P* values for a subset of promoters. It was determined that at $P < 0.001$ (which was considered significant for this study), there were an extremely high number of genes that bound both *Mnt* and *c-Myc* with similarly significant *P* values.

c-Myc bound 138 promoter sequences in one trial and 114 unique gene promoters in another trial whereas *Mnt* bound 147 of a possible 1,920 genes (Fig. 7*A-C*). When the 138 unique promoters of the first *c-Myc* location-analysis were compared with the 147 promoters from *Mnt*, 111 were found to be common (Fig. 7*D*). Of 114 unique promoters from the second *c-Myc* experiment, 84 were fond to be in common with the same set of *Mnt* bound genes (Fig. 7*E*). The *c-Myc* experiments yielded 80 common significantly bound promoters when compared with each other ($P < 0.001$). Of these genes, 75 were also found to bind *Mnt* at a significant level (Supplementary Table S2), indicating only 5 of the 80 genes were not bound by *Mnt* at a significant level (Fig. 7*F*). We validated these results with chromatin immunoprecipitation analysis of five genes that bound both Mnt and c-Myc, *Ibd1, Sap18, cdkn1b, Rab18*, and *Brca1*, showing that Mnt and c-Myc bound specifically to these promoters but not sequences 3′ to the transcriptional start site of these genes (Supplementary Fig. S1). These results show a significant overlap in promoter binding of *c-Myc* and *Mnt* in tumor tissue.

Expression analysis of genes preferentially bound by Mnt and c-Myc. If *Mnt* acts to regulate *c-Myc*, and the lack of Mnt results in tumorigenesis by removing a mechanism to counter *c-Myc* expression, we reasoned that there may be a similarity in gene expression between the two types of tumors. To test this hypothesis, we compared the expression of 45,000 genes in *MMTV-c-Myc* transgenic and $Mnt^{CKO/CKO}$; *MMTV-Cre* mammary tumors. The expression levels were analyzed using bioweight analysis, which is a combined measure of fold change and *P* values from *t* tests (30). This method has been shown to have more statistical power for small sample sets than traditional means of microarray analysis based on the *t* test. A large bioweight value suggests that the gene is likely to have a small *P* value, a large fold change, and is more likely to have statistically significant differences in expression. This allows one to rank order the genes from most to least similar in expression based on two methods of measurement. We were interested to see if the different tumors from *MMTV-c-Myc* and $Mnt^{CKO/CKO}$; *MMTV-Cre* mice show any similarity in gene expression pattern, indicated by a low bioweight value.

A volcano plot of the 45,000 genes indicates that there are very few genes with significant bioweights (Fig. 8), suggesting an overall expression pattern that is very similar between *c-Myc* transgenic and $MMTV\text{-}CRE^{+}/Mnt^{CKO/CKO}$ mammary tumors. In this plot, the *X* axis represents the across-replicate binary fold change between c-Myc transgenic and $MMTV\text{-}CRE^{+}/Mnt^{CKO/CKO}$. The *Y* axis represents the negative decimal log of *P* values for the gene specific *t* tests using the null hypothesis that the average log-ratios are zero (no difference between groups). The most statistically significant genes are located on the top left and top right boxed areas of the volcano plot. Left-to-right variability corresponds to a large absolute fold change. This method of measurement is able to represent the relationship between "biological" and "statistical" significance in one graph. Because only two genes are located in either of these boxes, the vast majority of genes are similarly expressed in tumors from c-Myc transgenic and $MMTV\text{-}CRE^{+}/Mnt^{CKO/CKO}$.

The 75 genes discovered to have similarly bound promoters using GWLA at $P \leq 0.001$ were then assessed. Many of these genes are of obvious biological relevance in tumorigenesis, cell cycle

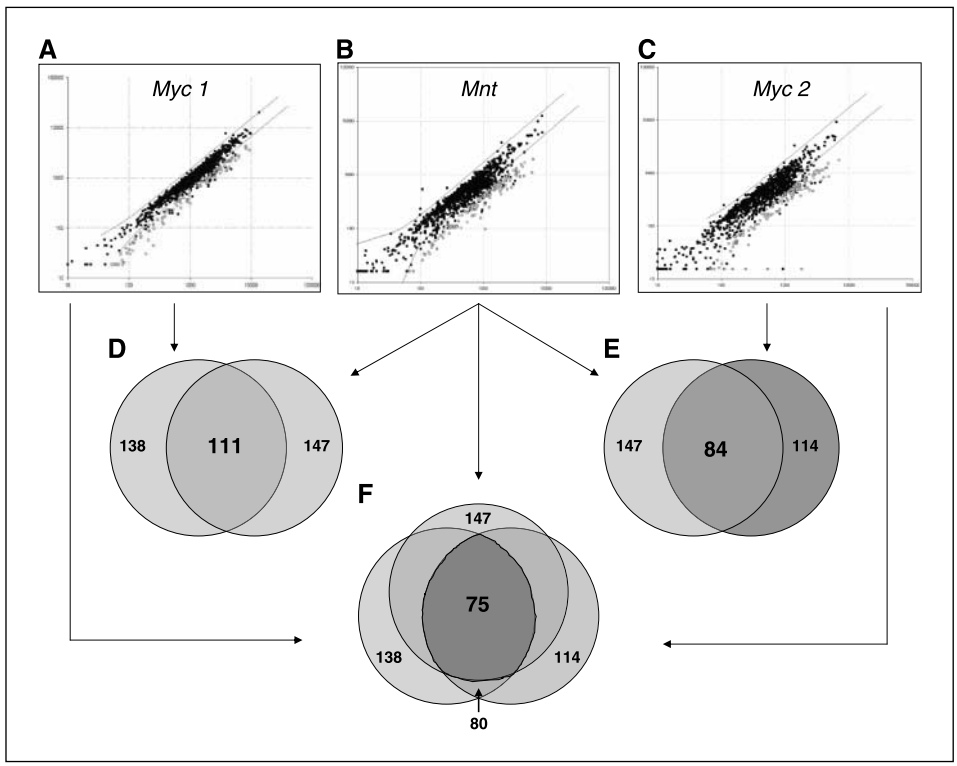

Figure 7. GWLA profiles of Myc and Mnt binding to M2K promoter arrays using tumors from *MMTV-c-Myc* transgenic mice and the overlap of significant binding. *A,* there were 138 promoters bound in one tumor sample by Myc at $P < 0.001$. *B,* Mnt bound 147 genes at a significant level; *C,* the second Myc bound 114 genes at a significant level. *D,* when Myc 1 binding is compared with Mnt, 111 genes were found to be common. Myc2 and Mnt shared 84 promoters (*E*) whereas Myc1 compared with Myc2 had 80 genes in common (*F*); all three combined shared 75 genes, indicating these 75 genes are probably biologically significant.

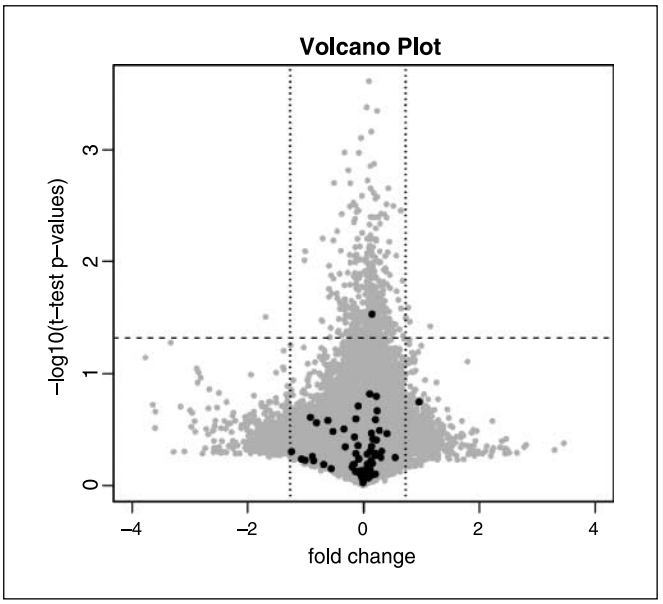

Figure 8. Bioweight analysis reveals a tight clustering of expression in both the ranges of *P* values and fold change in expression between *MMTV-c-Myc* transgenic and $Mnt^{CKO/CKO}$; *MMTV-Cre* tumors. *Gray-shaded points,* ~45,000 genes from the Affymetrix 430 2.0 mouse microarray chip. *Black-shaded points,* 75 genes identified by GWLA. *Horizontal dotted line, P* value significance threshold corresponding to a type I error rate of 0.05. *Vertical dotted lines,* fold change thresholds corresponding to a binary log fold difference of 1 and −1 (which is equivalent to an absolute regular fold change of 2). Genes significantly different between tumors from *MMTV-c-Myc* transgenic and $Mnt^{CKO/CKO}$; *MMTV-Cre* mice are in the top left and top right areas delineated by the dotted lines, and only two genes were in those quadrants. Of the 75 genes clustered tightly by GWLA, only one was expressed at a level above 1 binary log fold difference and another gene exceeded the *P* value threshold.

regulation, proliferation, and transcriptional regulation (data not shown; Supplementary Table S2). The bioweight values for these genes varied from 0.0001 to 0.73, with the majority decreasing below 0.2 (63 of 75 were below 0.2). These low values indicate that the overall expression pattern is similar between the tumor types and these directly regulated genes are not different in expression in mammary gland tumors resulting from loss of Mnt or overexpression of c-Myc.

Discussion

Elevated c-Myc expression is a common feature of human breast cancers (reviewed in ref. 34) and overexpression of c-Myc in mammary gland tissue of transgenic mice leads to mammary gland cancer (reviewed in ref. 35). Thus, mammary gland epithelial tissue offers an excellent model system to study the function of the putative Myc antagonist Mnt. Consistent with the proposed Myc-antagonist function of Mnt, we previously showed that deletion of Mnt specifically in mammary gland tissue using a Mnt conditional knockout led to the formation of adenocarcinomas (21). Here we show that Mnt also plays an important role in mammary gland development preceding tumor formation, as loss of Mnt impairs mammary gland involution. In addition, we further characterize tumor formation caused by loss of Mnt and show that the gene expression profiles of tumors that lack Mnt are similar to those caused by Myc overexpression.

The finding that loss of *Mnt* can lead to mammary gland tumorigenesis is consistent with our results showing that loss of *Mnt* causes a hyperproliferation phenotype in mouse embryonic fibroblasts, including accelerated proliferation, increased sensitivity to apoptosis, sensitivity to transformation by $H\text{-}Ras^{V12}$ alone, and senescence bypass (21). In both mouse embryonic fibroblasts and mammary gland tumors, loss of Mnt was found to cause up-regulation of cyclin E and Cdk4 (21), both of which have been implicated in mammary gland tumorigenesis (reviewed in ref. 36). Mnt has also been shown to preferentially bind similar promoter regions to c-Myc in mammary tumor tissues from c-Myc transgenic mice and the corresponding proteins were shown to be expressed at similar levels in both Mnt knockout and c-Myc transgenic tumors. Furthermore, because it is well established that c-Myc promotes mammary gland tumorigenesis in transgenic mice (33), these results are consistent with the proposed role of Mnt as a Myc antagonist and tumor suppressor.

Depending on the *in vivo* cellular context, dysregulation of c-Myc can either promote proliferation or induce apoptosis (37–39). Induction of apoptosis, and possibly induction of cell cycle arrest (40), likely provide protection against the proliferative effects of over-activity of Myc family proteins. Indeed, Myc-driven tumorigenesis is dramatically accelerated in mouse models when apoptosis is suppressed by expressing antiapoptotic proteins (39, 41–43) or by disruption of p53 pathway function (25, 43–47). Because, in general, cells are sensitized to apoptosis by Myc overexpression and we previously found apoptosis levels increased in fibroblasts lacking Mnt, it was predicted that loss of Mnt and its Myc-antagonistic activity would result in increased apoptosis in mammary gland tissue (21). However, just the opposite was observed during mammary gland involution (Fig. 3), a process characterized by high levels of apoptosis (48). It is possible that cell type differences in the response to loss of Mnt are responsible for this apparent discrepancy or that the decreased apoptosis is the result of impaired initiation of the involution process that precedes active apoptosis. Another possible explanation is that the observed decreased apoptosis is a secondary response to hyper-Myc activity caused by loss of Mnt. In the later scenario, decreased apoptosis during involution may be a manifestation of prior elimination—by apoptosis—of cells important for the involution process. Under such conditions, cells with innate or acquired resistance to apoptosis would have a selective advantage and perhaps are the precursors to tumors caused by loss of Mnt. In situations of Myc overexpression, variant cells less prone to apoptosis are selected that have disrupted ADP ribosylation factor (ARF)/murine double minute-2/p53 pathway function (25, 46, 49). Similarly, primary $Mnt^{-/-}$ fibroblasts seem to sustain p53 mutation or loss of ARF more rapidly than wild-type cells during serial passaging (21) and tumors arising from $MMTV\text{-}Cre^{+}/Mnt^{KO/CKO}$ mice express elevated p53, which is often indicative of disabling mutations in p53 (data not shown). Furthermore, there is a modest increase in p53 and p19ARF in the phenotypically normal mammary gland tissue of some $MMTV\text{-}Cre^{+}/Mnt^{KO/CKO}$ mice (data not shown), raising the possibility that the decrease in apoptosis during involution is associated with the evolution of cells in mammary gland tissue that have sustained mutations in the *p53* gene. Interestingly, $p53^{-/-}$ mice on a BALB/c genetic background exhibit a delayed involution phenotype and develop mammary tumors (50). The role of the ARF/murine double minute-2/p53 pathway and suppression of apoptosis in tumor formation by $MMTV\text{-}Cre^{+}/Mnt^{KO/CKO}$ mice can be tested by determining whether mammary gland tumor formation in the absence of Mnt is accelerated by, for example, loss of ARF or p53 or by overexpression of Bcl-2 or other antiapoptotic proteins.

We found that mice with multiple pregnancies had a higher percentage of enlarged ducts and larger average size of ductal lumen than *MMTV-Cre*$^{+}$/*Mnt*$^{KO/CKO}$ virgin mice (Fig. 4). The accumulation of apoptotic defects in the involution of each pregnancy may be part of the reason for causing the enlargement of mammary ducts. However, virgin *MMTV-Cre*$^{+}$/*Mnt*$^{KO/CKO}$ mice showed higher percentage of enlarged ducts than virgin wild-type mice. This result suggests that there are other causes than the accumulation of apoptotic defects. Hyperproliferation of the ductal epithelial cells may be a possible explanation but we could not detect any difference in proliferating cell nuclear antigen expression between *MMTV-Cre*$^{+}$/*Mnt*$^{KO/CKO}$ mice and wild-type mice (data not shown). Although no changes were noted in levels of Mnt expression during mammary gland development, c-Myc levels varied greatly during mammary gland development. Thus, in the absence of Mnt, these changes in c-Myc will be unopposed and may lead to the developmental defects observed.

Similar promoter binding of *c-Myc* and *Mnt* in *c-Myc* mammary tumors (Fig. 7) supports the hypothesis that Mnt may be an important direct regulator of c-Myc *in vivo* by competing with c-Myc for binding to Max and shared target genes. Although the Mad protein family may be important in this regulation under certain conditions, evidence presented here, as well as data showing concurrent expression of c-Myc and Mnt in dividing cells (21), suggests that Mnt antagonism may be particularly relevant to the control of cell proliferation. In addition, our results suggest that global gene expression is virtually indistinguishable in tumors of *c-Myc* transgenic mice and tumors of *Mnt*$^{KO/CKO}$*; MMTV-Cre* conditional knockout mice (Fig. 8). Taken together with previous cell culture studies (21), these findings support the hypothesis that *Mnt* acts in direct functional opposition to *c-Myc* in regulating transcription and that loss of Mnt is, to a large extent, functionally equivalent to elevated and/or deregulated c-Myc expression.

It is known that the MMTV promoter contains a hormonal regulatory element, which can be induced by progesterone, glucocorticoids, androgens, and prolactin (51–53). We have continuously mated *MMTV-Cre*$^{+}$/*Mnt*$^{KO/CKO}$ mice to promote the expression of *Cre* transgene. There are many reports that hormones are important factors to alter mammary tumor development (54–56). Unlike female *MMTV-Cre*$^{+}$/*Mnt*$^{KO/CKO}$ mice, male mice did not develop mammary tumors (data not shown). Male *MMTV-Cre*$^{+}$/*Mnt*$^{KO/CKO}$ mice might develop mammary tumors after the administration of hormones and may be a good tool to analyze the effect of hormones in the development of mammary tumors in *MMTV-Cre*$^{+}$/*Mnt*$^{KO/CKO}$ mice. However, it remains to be determined whether hormones have a role in Myc/Mnt signaling or only affect the direct *Cre* transgene induction in *MMTV-Cre*$^{+}$/*Mnt*$^{KO/CKO}$ mice.

We also produced mice with a null mutation of *Mnt* using the conditional allele and germ line Cre deleter strains (21, 23). Almost all homozygous mutants (*Mnt*$^{-/-}$) in a mixed or inbred genetic background died perinatally. Of the <2% of *Mnt*$^{-/-}$ mice in a mixed genetic background and ~3.5% *Mnt*$^{-/-}$ mice in an inbred background that survived to adulthood, all died within 1 year and most of these died within several months of birth from currently unknown causes. Therefore, it has not been possible to address whether mice completely deficient for *Mnt* develop mammary gland cancers and/or other tumors and we have not detected any tumors in *Mnt* heterozygotes. Thus, *Mnt* conditional knockout mice will be required to address the possibility that Mnt functions as a tumor suppressor in other cell types and to determine whether *MNT* is the tumor suppressor or one of the general tumor suppressors suspected to reside at human chromosome 17p13.3 (57, 58).

Acknowledgments

Received 8/2/2005; revised 3/1/2006; accepted 3/22/2006.

The costs of publication of this article were defrayed in part by the payment of page charges. This article must therefore be hereby marked *advertisement* in accordance with 18 U.S.C. Section 1734 solely to indicate this fact.

We thank Hideki Wanibuchi for helpful discussions.

References

1. Grandori C, Cowley SM, James LP, Eisenman RN. The Myc/Max/Mad network and the transcriptional control of cell behavior. Annu Rev Cell Dev Biol 2000;16:653–99.
2. Nesbit CE, Tersak JM, Prochownik EV. MYC oncogenes and human neoplastic disease. Oncogene 1999; 18:3004–16.
3. Stewart TA, Pattengale PK, Leder P. Spontaneous mammary adenocarcinomas in transgenic mice that carry and express MTV/myc fusion genes. Cell 1984;38: 627–37.
4. Schoenenberger CA, Andres AC, Groner B, van der Valk M, LeMeur M, Gerlinger P. Targeted c-myc gene expression in mammary glands of transgenic mice induces mammary tumours with constitutive milk protein gene transcription. EMBO J 1988;7:169–75.
5. Leder A, Pattengale PK, Kuo A, Stewart TA, Leder P. Consequences of widespread deregulation of the c-myc gene in transgenic mice: multiple neoplasms and normal development. Cell 1986;45:485–95.
6. Walker W, Zhou ZQ, Ota S, Wynshaw Boris A, Hurlin PJ. Mnt-Max to Myc-Max complex switching regulates cell cycle entry. J Cell Biol 2005;169:405–13.
7. Devilee P, Cornelisse CJ. Somatic genetic changes in human breast cancer. Biochim Biophys Acta 1994;1198: 113–30.
8. McDonald JD, Daneshvar L, Willert JR, Matsumura K, Waldman F, Cogen PH. Physical mapping of chromosome 17p13.3 in the region of a putative tumor suppressor gene important in medulloblastoma. Genomics 1994;23:229–32.
9. Williamson MP, Elder PA, Knowles MA. The spectrum of TP53 mutations in bladder carcinoma. Genes Chromosomes Cancer 1994;9:108–18.
10. Biegel JA, Burk CD, Barr FG, Emanuel BS. Evidence for a 17p tumor related locus distinct from p53 in pediatric primitive neuroectodermal tumors. Cancer Res 1992;52:3391–5.
11. Takahashi T, Konishi H, Kozaki K, et al. Molecular analysis of a Myc antagonist, ROX/Mnt, at 17p13.3 in human lung cancers. Jpn J Cancer Res 1998;89:347–51.
12. Sommer A, Waha A, Tonn J, et al. Analysis of the Max-binding protein MNT in human medulloblastomas. Int J Cancer 1999;82:810–6.
13. Nigro CL, Venesio T, Reymond A, et al. The human ROX gene: genomic structure and mutation analysis in human breast tumors. Genomics 1998;49:275–82.
14. Hirano A, Emi M, Tsuneizumi M, et al. Allelic losses of loci at 3p25.1, 8p22, 13q12, 17p13.3, and 22q13 correlate with postoperative recurrence in breast cancer. Clin Cancer Res 2001;7:876–82.
15. Fujii H, Biel MA, Zhou W, Weitzman SA, Baylin SB, Gabrielson E. Methylation of the HIC-1 candidate tumor suppressor gene in human breast cancer. Oncogene 1998;16:2159–64.
16. Morton RA, Jr., Watkins JJ, Bova GS, Wales MM, Baylin SB, Isaacs WB. Hypermethylation of chromosome 17P locus D17S5 in human prostate tissue. J Urol 1996; 156:512–6.
17. Wales MM, Biel MA, el Deiry W, et al. p53 activates expression of HIC-1, a new candidate tumour suppressor gene on 17p13.3. Nat Med 1995;1:570–7.
18. Chen WY, Zeng X, Carter MG, et al. Heterozygous disruption of Hic1 predisposes mice to a gender-dependent spectrum of malignant tumors. Nat Genet 2003;33:197–202.
19. Cvekl A, Jr., Zavadil J, Birshtein BK, Grotzer MA, Cvekl A. Analysis of transcripts from 17p13.3 in medulloblastoma suggests ROX/MNT as a potential tumour suppressor gene. Eur J Cancer 2004;40:2525–32.
20. Dobyns WB, Reiner O, Carrozzo R, Ledbetter DH. Lissencephaly. A human brain malformation associated with deletion of the LIS1 gene located at chromosome 17p13. JAMA 1993;270:2838–42.
21. Hurlin PJ, Zhou Z-Q, Toyo-oka K, et al. Deletion of Mnt leads to disrupted cell cycle control and tumorigenesis. EMBO J 2003;22:1–13.
22. Nilsson JA, Cleveland JL. Mnt: master regulator of the Max network. Cell Cycle 2004;3:588–90.
23. Toyo-oka K, Hirotsune S, Gambello MJ, et al. Loss of the Max-interacting protein Mnt in mice results in decreased viability, defective embryonic growth and craniofacial defects: relevance to Miller-Dieker syndrome. Hum Mol Genet 2004;13:1057–67.
24. Lakso M, Pichel JG, Gorman JR, et al. Efficient *in vivo* manipulation of mouse genomic sequences at the zygote stage. Proc Natl Acad Sci U S A 1996;93:5860–5.
25. Eischen CM, Weber JD, Roussel MF, Sherr CJ, Cleveland JL. Disruption of the ARF-Mdm2-53 tumor

suppressor pathway in Myc-induced lymphomagenesis. Genes Dev 1999;13:2658–69.
26. Hurlin PJ, Steingrimsson E, Copeland NG, Jenkins NA, Eisenman RN. Mga, a dual-specificity transcription factor that interacts with Max and contains a T-domain DNA-binding motif. EMBO J 1999;18:7019–28.
27. Metivier R, Penot G, Hubner MR, et al. Estrogen receptor-α directs ordered, cyclical, and combinatorial recruitment of cofactors on a natural target promoter. Cell 2003;115:751–63.
28. Li Z, Van Calcar S, Qu C, Cavenee WK, Zhang MQ, Ren B. A global transcriptional regulatory role for c-Myc in Burkitt's lymphoma cells. Proc Natl Acad Sci U S A 2003;100:8164–9.
29. Irizarry RA, Bolstad BM, Collin F, Cope LM, Hobbs B, Speed TP. Summaries of Affymetrix GeneChip probe level data. Nucleic Acids Res 2003;31:e15.
30. Rosenfeld S, Wang T, Kim Y, Milner J. Numerical deconvolution of cDNA microarray signal: simulation study. Ann N Y Acad Sci 2004;1020:110–23.
31. Xu X, Wagner KU, Larson D, et al. Conditional mutation of Brca1 in mammary epithelial cells results in blunted ductal morphogenesis and tumour formation. Nat Genet 1999;22:37–43.
32. Wagner KU, Wall RJ, St Onge L, et al. Cre-mediated gene deletion in the mammary gland. Nucleic Acids Res 1997;25:4323–30.
33. Hutchinson JN, Muller WJ. Transgenic mouse models of human breast cancer. Oncogene 2000;19:6130–7.
34. Liao DJ, Dickson RB. c-Myc in breast cancer. Endocr Relat Cancer 2000;7:143–64.
35. Amundadottir LT, Merlino G, Dickson RB. Transgenic mouse models of breast cancer. Breast Cancer Res Treat 1996;39:119–35.
36. Landberg G. Multiparameter analyses of cell cycle regulatory proteins in human breast cancer: a key to definition of separate pathways in tumorigenesis. Adv Cancer Res 2002;84:35–56.
37. Pelengaris S, Littlewood T, Khan M, Elia G, Evan G. Reversible activation of c-Myc in skin: induction of a complex neoplastic phenotype by a single oncogenic lesion. Mol Cell 1999;3:565–77.
38. Pelengaris S, Khan M, Evan G. c-MYC: more than just a matter of life and death. Nat Rev Cancer 2002;2:764–76.
39. Pelengaris S, Khan M, Evan GI. Suppression of Myc-induced apoptosis in β cells exposes multiple oncogenic properties of Myc and triggers carcinogenic progression. Cell 2002;109:321–34.
40. Felsher DW, Zetterberg A, Zhu J, Tlsty T, Bishop JM. Overexpression of MYC causes p53-dependent G_2 arrest of normal fibroblasts. Proc Natl Acad Sci U S A 2000;97:10544–8.
41. Strasser A, Harris AW, Bath ML, Cory S. Novel primitive lymphoid tumours induced in transgenic mice by cooperation between myc and bcl-2. Nature 1990;348:331–3.
42. Jager R, Herzer U, Schenkel J, Weiher H. Overexpression of Bcl-2 inhibits alveolar cell apoptosis during involution and accelerates c-myc-induced tumorigenesis of the mammary gland in transgenic mice. Oncogene 1997;15:1787–95.
43. Jacobs JJ, Scheijen B, Voncken JW, Kieboom K, Berns A, van Lohuizen M. Bmi-1 collaborates with c-Myc in tumorigenesis by inhibiting c-Myc-induced apoptosis via INK4a/ARF. Genes Dev 1999;13:2678–90.
44. Blyth K, Terry A, O'Hara M, et al. Synergy between a human c-myc transgene and p53 null genotype in murine thymic lymphomas: contrasting effects of homozygous and heterozygous p53 loss. Oncogene 1995;10:1717–23.
45. Elson A, Deng C, Campos Torres J, Donehower LA, Leder P. The MMTV/c-myc transgene and p53 null alleles collaborate to induce T-cell lymphomas, but not mammary carcinomas in transgenic mice. Oncogene 1995;11:181–90.
46. Schmitt CA, McCurrach ME, de Stanchina E, Wallace Brodeur RR, Lowe SW. INK4a/ARF mutations accelerate lymphomagenesis and promote chemoresistance by disabling p53. Genes Dev 1999;13:2670–7.
47. Eischen CM, Rehg JE, Korsmeyer SJ, Cleveland JL. Loss of Bax alters tumor spectrum and tumor numbers in ARF-deficient mice. Cancer Res 2002;62:2184–91.
48. Walker NI, Bennett RE, Kerr JF. Cell death by apoptosis during involution of the lactating breast in mice and rats. Am J Anat 1989;185:19–32.
49. Zindy F, Eischen CM, Randle DH, et al. Myc signaling via the ARF tumor suppressor regulates p53-dependent apoptosis and immortalization. Genes Dev 1998;12:2424–33.
50. Blackburn AC, Jerry DJ. Knockout and transgenic mice of Trp53: what have we learned about p53 in breast cancer? Breast Cancer Res 2002;4:101–11.
51. Darbre P, Dickson C, Peters G, Page M, Curtis S, King RJ. Androgen regulation of cell proliferation and expression of viral sequences in mouse mammary tumour cells. Nature 1983;303:431–3.
52. Chalepakis G, Arnemann J, Slater E, Bruller HJ, Gross B, Beato M. Differential gene activation by glucocorticoids and progestins through the hormone regulatory element of mouse mammary tumor virus. Cell 1988;53:371–82.
53. Haraguchi S, Good RA, Engelman RW, Day NK. Human prolactin regulates transfected MMTV LTR-directed gene expression in a human breast-carcinoma cell line through synergistic interaction with steroid hormones. Int J Cancer 1992;52:928–33.
54. Cavalieri EL, Stack DE, Devanesan PD, et al. Molecular origin of cancer: catechol estrogen-3,4-quinones as endogenous tumor initiators. Proc Natl Acad Sci U S A 1997;94:10937–42.
55. Fisher B, Costantino JP, Wickerham DL, et al. Tamoxifen for prevention of breast cancer: report of the National Surgical Adjuvant Breast and Bowel Project P-1 Study. J Natl Cancer Inst 1998;90:1371–88.
56. Yang X, Edgerton SM, Kosanke SD, et al. Hormonal and dietary modulation of mammary carcinogenesis in mouse mammary tumor virus-c-erbB-2 transgenic mice. Cancer Res 2003;63:2425–33.
57. Hurlin PJ, Queva C, Eisenman RN. Mnt, a novel Max-interacting protein is coexpressed with Myc in proliferating cells and mediates repression at Myc binding sites. Genes Dev 1997;11:44–58.
58. Meroni G, Reymond A, Alcalay M, et al. Rox, a novel bHLHZip protein expressed in quiescent cells that heterodimerizes with Max, binds a non-canonical E box and acts as a transcriptional repressor. EMBO J 1997;16:2892–906.

Correction

Mnt Is a Tumor Suppressor in Mammary Gland

In the article on how Mnt is a tumor suppressor in mammary gland in the June 1, 2006 issue of *Cancer Research* (1), the correct spelling of the seventh author's name is Laure Escoubet-Lozach and the correct spelling of the eighth author's name is Ivan Garcia-Bassets. Also, the affiliation for Christopher K. Glass should have been listed as the Department of Cellular and Molecular Medicine, Ludwig Cancer Institute, and the Department of Medicine, University of California, San Diego School of Medicine, La Jolla, California.

1. Toyo-oka K, Bowen TJ, Hirotsune S, Li Z, Jain S, Ota S, Escoubet-Lozach L, Garcia-Bassets I, Lozach J, Rosenfeld MG, Glass CK, Eisenman R, Ren B, Hurlin P, Wynshaw-Boris A. Mnt-deficient mammary glands exhibit impaired involution and tumors with characteristics of Myc Overexpression. Cancer Res 2006;66:5565–73.

doi:10.1158/0008-5472.CAN-66-13-COR2

Mnt-Deficient Mammary Glands Exhibit Impaired Involution and Tumors with Characteristics of Myc Overexpression

Kazuhito Toyo-oka, Timothy J. Bowen, Shinji Hirotsune, et al.

Cancer Res 2006;66:5565-5573.